

Composition-induced structural instability and strong-coupling superconductivity in $\text{Au}_{1-x}\text{Pd}_x\text{Te}_2$

Kazutaka Kudo,^{1,2,*} Hiroyuki Ishii,¹ and Minoru Nohara^{1,2,†}

¹*Department of Physics, Okayama University, Okayama 700-8530, Japan*

²*Research Institute for Interdisciplinary Science, Okayama University, Okayama 700-8530, Japan*

(Dated:)

The physical properties and structural evolution of the MX_2 -type solid solution $\text{Au}_{1-x}\text{Pd}_x\text{Te}_2$ are reported. The end member AuTe_2 is a normal metal with a monoclinic distorted CdI_2 -type structure with preformed Te–Te dimers. A monoclinic–trigonal structural phase transition at a finite temperature occurs upon Pd substitution and is suppressed to zero temperature near $x = 0.55$, and a superconducting phase with a maximum $T_c = 4.65$ K emerges. A clear indication of strong coupling superconductivity is observed near the composition of the structural instability. The competitive relationship between Te–Te dimers and superconductivity is proposed.

PACS numbers: 74.70.Dd, 74.25.Dw, 74.25.-q, 74.25.Bt

Superconductivity at a relatively high transition temperature (T_c) often emerges near structural instability that is characterized by pressure- or composition-induced structural phase transition. Typical examples of such superconductivity are of iron and nickel pnictides [1–6], iridium and gold tellurides [1, 7–11], A15 compounds [13], graphite intercalated compounds [14, 15], and quasiskutterudite stanides [16–18]. Among them, iridium and gold tellurides, namely IrTe_2 and AuTe_2 with distorted CdI_2 -type structures, have been attracting considerable interest because their structural instabilities result from the breaking of moleculelike dimers of iridium [19, 20] or tellurium [1, 11], and the subsequent emergence of a superconducting phase upon applying hydrostatic pressure [1] or chemical doping [7–11]. The evolution of electronic states across the structural transition has been intensively studied on IrTe_2 [21–24], while the study of AuTe_2 is limited [25] because composition-induced structural instability has not yet been exhibited experimentally.

AuTe_2 , known as mineral calaverite, crystallizes in a monoclinic distorted CdI_2 -type structure with the space group $C2/m$ (C_{2h}^3 , No. 12) [26]. Each AuTe_2 layer consists of edge-shared AuTe_6 octahedra that are strongly distorted with two short (2.67 Å) and four long (2.98 Å) Au–Te bonds in the average structure [26]. This is due to the formation of Te–Te dimers with a bond length of 2.88 Å between the layers [27], which results in an incommensurate modulation of $\mathbf{q} = -0.4076\mathbf{a}^* + 0.4479\mathbf{c}^*$. Recently, Kitagawa *et al.* demonstrated that AuTe_2 exhibits pressure-induced structural instability that is characterized by a monoclinic–trigonal structural phase transition, together with the subsequent emergence of a superconducting phase with a maximum $T_c = 2.3$ K [1]. Kudo *et al.* reported superconductivity at $T_c = 4.0$ K in the solid solution $\text{Au}_{1-x}\text{Pt}_x\text{Te}_2$ with $x = 0.35$ [11]. In both cases, superconductivity emerges in the undistorted trigonal CdI_2 -type structure with the space group $P\bar{3}m1$ (D_{3d}^3 , No. 164) [1, 11, 28], where Te–Te dimers are broken. However, the pronounced phase separation that

occurs at $1.6 < P < 2.7$ GPa in AuTe_2 under pressure [1] or $0.1 < x < 0.15$ in the solid solution $\text{Au}_{1-x}\text{Pt}_x\text{Te}_2$ [11] has inhibited us from accessing the critical region of structural instability. Thus, we should search for another doping element that forms continuous solid solution in AuTe_2 .

In this paper, we report on the physical properties and structural evolution of $\text{Au}_{1-x}\text{Pd}_x\text{Te}_2$, which forms continuous solid solution across structural instability. We demonstrate the systematic suppression of the monoclinic Te–Te dimer phase of AuTe_2 by Pd substitution. A superconducting phase emerges when the monoclinic phase is suppressed and the trigonal phase appears at $x = 0.55$. The specific heat and magnetization data suggest that the enhanced electronic density of states (DOS) at the Fermi level E_F is responsible for the observed strong-coupling superconductivity. On the other hand, the DOS at E_F is strongly suppressed in the monoclinic phase, suggesting the competition between Te–Te dimers and superconductivity. Our finding demonstrates that the breaking of moleculelike dimers in solids offers a novel route to develop superconductors.

Polycrystalline samples of $\text{Au}_{1-x}\text{Pd}_x\text{Te}_2$ with nominal compositions of $0.00 \leq x \leq 1.00$ were synthesized using a solid-state reaction. First, stoichiometric amounts of Au (99.99%), Pd (99.98%), and Te (99.99%) were mixed and pulverized. They were heated at 500°C for 24 h in an evacuated quartz tube. Subsequently, the product was powdered, pressed into pellets, and annealed at 350–700°C for 24 h in an evacuated quartz tube. The annealing was performed once or twice to homogenize the sample. The heating and cooling rates both equaled 20°C/h. The resulting samples were characterized at room temperature by powder x-ray diffraction (XRD) using a Rigaku RINT-TTR III x-ray diffractometer with Cu $K\alpha$ radiation and were identified to be a single phase of $\text{Au}_{1-x}\text{Pd}_x\text{Te}_2$ [29]. Energy dispersive x-ray spectrometry (EDS) was used to determine the x . The measured x values were in good agreement with the nominal ones;

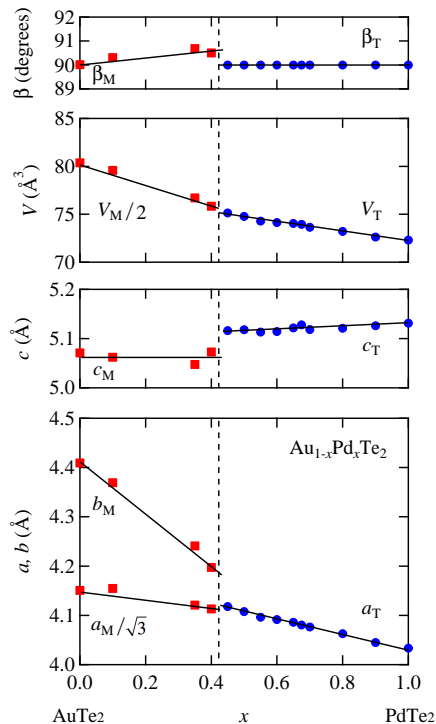


FIG. 1. Room-temperature lattice parameters for $\text{Au}_{1-x}\text{Pd}_x\text{Te}_2$. Subscripts M and T respectively indicate monoclinic and trigonal phases.

we used the nominal x in this study. Magnetization M was measured using a Quantum Design magnetic property measurement system (MPMS). Electrical resistivity ρ and specific heat C were measured using a Quantum Design physical property measurement system (PPMS).

The structural instability that results from Te–Te dimer breaking, which can be recognized as the structural transition from a monoclinic to trigonal phase, was observed at $x = 0.4$ at room temperature, as shown in Fig. 1. The XRD profiles for $x \leq 0.40$ can be indexed based on the monoclinic average structure of end-member AuTe_2 ; as the Pd content increases, the parameters a and b decrease, while the parameter c shows no substantial change. Between $x = 0.40$ and 0.45 , the structural phase transition to a trigonal phase occurs, indicating the breaking of Te–Te dimers by Pd doping. The discontinuous changes in the lattice parameters suggest a first-order phase transition. The parameter a slightly increases, the parameter b decreases, and the parameter c increases. Therefore, the resulting change in cell volume V is small.

The structural transition also depends on temperature. As is shown in Fig. 2, the temperature dependence of magnetization shows drops at 350 K for $x = 0.40$ and 240 K for $x = 0.45$, respectively, suggesting the reduction of the DOS at E_F . The drops in M/H is one order

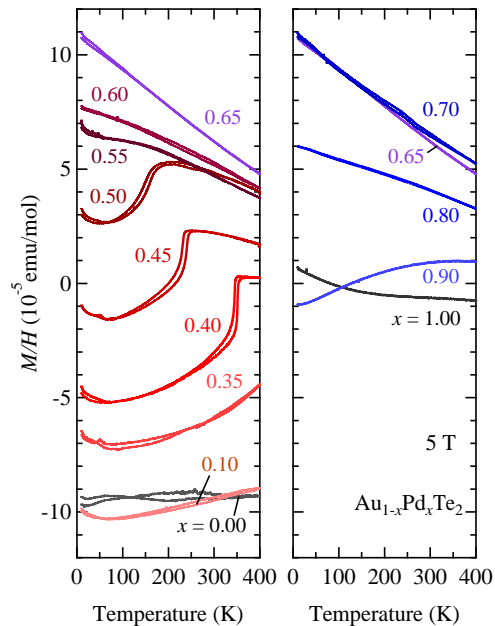


FIG. 2. Temperature dependence of magnetization divided by magnetic field, M/H , in the magnetic field of 5 T for $\text{Au}_{1-x}\text{Pd}_x\text{Te}_2$. Data were measured upon heating and cooling. The core diamagnetism for Pd, Au, and Te has not been corrected.

of magnitude smaller than those in systems that exhibit a metal–insulator transition [32]. In response to this, the electrical resistivity exhibits a jump at the same temperature, but it remains metallic at low temperatures (see Supplemental Material A [33]). The anomalies can be ascribable to the trigonal-to-monoclinic phase transition resulted from the formation of Te–Te dimers upon cooling, because the samples of $x = 0.40$ and 0.45 are identified as the monoclinic and trigonal phases, respectively, at room temperature, as shown in Fig. 1. The observed thermal hysteresis in the temperature dependence of magnetization and resistivity is consistent with the first-order phase transition, which is implied by the x dependence of the lattice parameters. We determined the structural phase transition temperature (T_s) from the drops in magnetization and jumps in resistivity. The T_s decreases with increasing Pd content and becomes absent at $x \geq 0.55$, suggesting that the isolated Te is stabilized down to $T = 0$ K in the compositions.

Along with the disappearance of Te–Te dimers, a superconducting phase appears. As shown in Fig. 3, the clear jump of the electronic specific heat (C_e) indicates the emergence of bulk superconductivity for $x \geq 0.55$, while the smeared jumps at $x = 0.45$ and 0.50 indicate the absence of bulk superconductivity in these samples. The maximum T_c of 4.65 K is observed at $x = 0.60$, and further Pd doping lowers T_c towards 1.69 K of $x = 1.00$

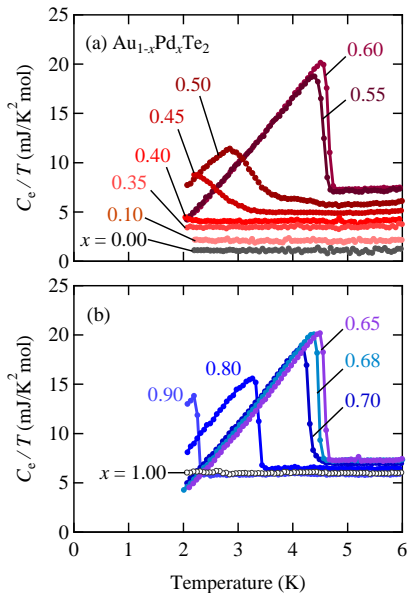


FIG. 3. Temperature dependence of electronic specific heat divided by temperature, C_e/T , for $\text{Au}_{1-x}\text{Pd}_x\text{Te}_2$, in which C_e is the difference of total specific heat C and phonon contribution.

[34]. The normalized specific-heat-jump at the superconducting transition ($\Delta C/\gamma T_c$) is 1.50 for $x = 0.90$ which agrees with the Bardeen-Cooper-Schrieffer (BCS) weak-coupling value of 1.43, whereas $\Delta C/\gamma T_c \simeq 1.94$ for $x \sim 0.60$ which corresponds to the value of strong electron-phonon coupling superconductors [35]. The superconducting transitions were also demonstrated by the sharp resistivity transition and the full shielding diamagnetic signal (see Supplemental Material B [33]).

The strong-coupling superconductivity observed in Pd-doped AuTe_2 is attributed to the enhanced DOS at E_F . Theoretically, either DOS enhancement or phonon softening can increase electron-phonon coupling [36]. However, a standard analysis of the low-temperature specific-heat data indicates that the phonon softening in the material is very small. The normal-state heat capacity data under an applied field that suppresses superconductivity is well fitted by equation $C/T = \gamma + \beta T^2$, as shown in Fig. 4, where γ is the electronic specific-heat coefficient and β is the phonon contribution. According to Fig. 5(a), estimated Debye temperature Θ_D exhibits little change ($< 5\%$) as a function of x , even though the system approaches the structural phase boundary. On the other hand, γ increases with decreasing Pd content in the trigonal side and achieves a maximum at the x where T_c exhibits the maximum value, as shown in Fig. 5(b). This is consistent with the magnetization data; the M/H of PdTe_2 ($x = 1.00$) is almost zero and the value rapidly increases with decreasing Pd content in the trigonal side,

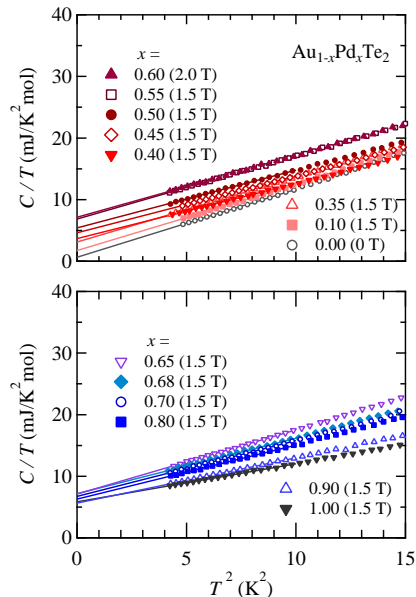


FIG. 4. The specific heat divided by temperature, C/T , as a function of T^2 for $\text{Au}_{1-x}\text{Pd}_x\text{Te}_2$. Solid lines denote fitted equation $C/T = \gamma + \beta T^2$, where γ is the electronic specific-heat coefficient and β is a constant that corresponds to the Debye phonon contribution.

as shown in Figs. 2 and 5(b). Thus, the magnetization and specific-heat results indicate that the strong-coupling superconductivity in the present system is exclusively attributed to the electronic origin. This highly contrasts with BaNi_2As_2 , in which strong-coupling superconductivity is accompanied by a drastic phonon softening ($> 30\%$) with no visible enhancement in the DOS [5].

Our results are summarized in Fig. 5. The monoclinic Te-Te dimer phase in AuTe_2 is suppressed by Pd doping, and vanishes at $x_c = 0.55$, as shown in Fig. 5(d). As soon as the Te-Te dimers disappear, a superconducting phase emerges in the trigonal phase, suggesting the competitive relationship between Te-Te dimers and superconductivity. This competition is ascribable to the reduction of DOS at E_F , because the γ and M/H in the monoclinic phase are strongly suppressed, as shown in Fig. 5(b). On the other hand, the strong-coupling superconductivity results from the enhanced DOS in the trigonal phase, as shown in Figs. 5(b) and 5(c). Both γ and M/H exhibit a broad maximum at $x_m \simeq 0.65$, which is noticeably apart from the monoclinic-trigonal phase boundary. The maximum is prominent in the x -dependent M/H at 10 K and $x \geq 0.55$ and even at 400 K and $x \geq 0.40$ in the trigonal phase, as shown in Fig. 5(b). Here, we note that the Wilson ratio $\Delta\chi/\gamma$ (in units of $3\mu_B^2/\pi^2 k_B^2$) at x_m , in which $\Delta\chi$ corresponds to the difference in M/H between $x = 0.00$ and $x = 0.65$ at 10

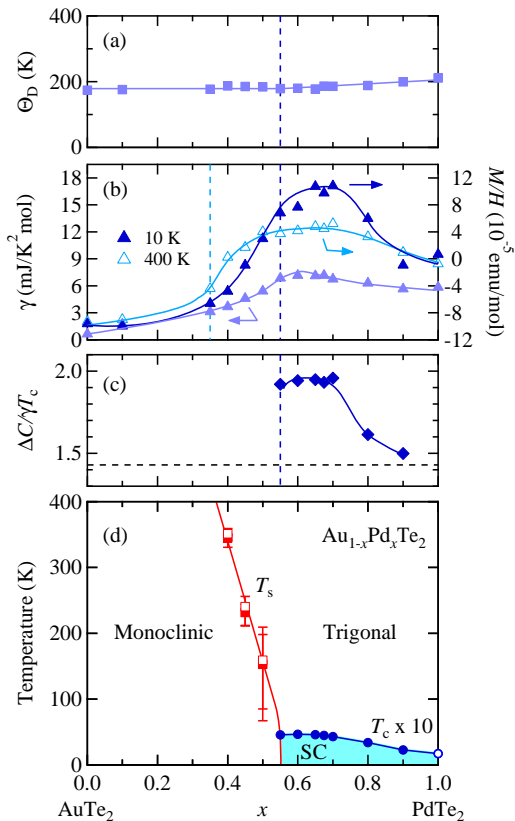


FIG. 5. (a) Debye temperature Θ_D , (b) electronic specific-heat coefficient γ and magnetic susceptibility M/H with temperature 10 and 400 K, and (c) normalized specific heat jump $\Delta C/\gamma T_c$ at the superconducting transition as a function of x for $\text{Au}_{1-x}\text{Pd}_x\text{Te}_2$, in which the horizontal dotted line corresponds to a BCS weak-coupling value of $\Delta C/\gamma T_c = 1.43$. (d) Electronic phase diagram of $\text{Au}_{1-x}\text{Pd}_x\text{Te}_2$, in which the (blue) closed circles represent the superconducting transition temperatures, T_c for $0.55 \leq x \leq 0.90$, that were determined from the specific heat measurements, and the (blue) open circle indicates T_c for $x = 1.00$ provided by Ref. 34. SC denotes the superconducting phase, and the (red) closed and open squares represent the trigonal-to-monoclinic structural phase transition temperatures, T_s , determined from the magnetization measurements upon cooling and heating, respectively. The solid curves are guides.

K, is estimated to be 2.0 [37]. This value could suggest the enhanced electronic correlation around x_m (see Supplemental Material C [33]). The remarkable increase in M/H caused by lowering temperature as well as the unusual T -linear temperature dependence in M/H for $x = 0.65$, shown in Fig. 2, might also suggest it. To address this issue, detailed investigation is expected with consideration for a possible proximity to a van Hove singularity, which is associated with the doping-dependent DOS maximum [1, 38, 39], as well as the structural instability that results from Te–Te dimer breaking.

In conclusion, our experiments demonstrate the emergence of strong-coupling superconductivity, which is associated with the enhancement of the electronic density of states in palladium-doped AuTe_2 . The superconductivity sets in as soon as the breaking of Te–Te dimers. The revealed competition between Te–Te dimers and superconductivity in the present system suggests that dimer breaking would invoke novel superconductivity in a wide variety of materials.

Some of this research was performed at the Advanced Science Research Center, Okayama University. This work was partially supported by Grants-in-Aid for Scientific Research (Grants No. 25400372, No. 26287082, No. 15H01047, and No. 15H05886) provided by the Japan Society for the Promotion of Science (JSPS).

* kudo@science.okayama-u.ac.jp

† nohara@science.okayama-u.ac.jp

- [1] C. de la Cruz, Q. Huang, J. W. Lynn, J. Li, W. Ratcliff II, J. L. Zarestky, H. A. Mook, G. F. Chen, J. L. Luo, N. L. Wang, and P. Dai, *Nature (London)* **453**, 899 (2008).
- [2] J. L. Niedziela, D. Parshall, K. A. Lokshin, A. S. Sefat, A. Alatas, and T. Egami, *Phys. Rev. B* **84**, 224305 (2011).
- [3] T. Goto, R. Kurihara, K. Araki, K. Mitsumoto, M. Akatsu, Y. Nemoto, S. Tatematsu, and M. Sato, *J. Phys. Soc. Jpn.* **80**, 073702 (2011).
- [4] M. Yoshizawa, D. Kimura, T. Chiba, S. Simayi, Y. Nakanishi, K. Kihou, C.-H. Lee, A. Iyo, H. Eisaki, M. Nakajima, and S. Uchida, *J. Phys. Soc. Jpn.* **81**, 024604 (2012).
- [5] K. Kudo, M. Takasuga, Y. Okamoto, Z. Hiroi, and M. Nohara, *Phys. Rev. Lett.* **109**, 097002 (2012).
- [6] D. Hirai, F. von Rohr, and R. J. Cava, *Phys. Rev. B* **86**, 100505(R) (2012).
- [7] S. Pyon, K. Kudo, and M. Nohara, *J. Phys. Soc. Jpn.* **81**, 053701 (2012).
- [8] J. J. Yang, Y. J. Choi, Y. S. Oh, A. Hogan, Y. Horibe, K. Kim, B. I. Min, and S-W. Cheong, *Phys. Rev. Lett.* **108**, 116402 (2012).
- [9] M. Kamitani, M. S. Bahramy, R. Arita, S. Seki, T. Arima, Y. Tokura, and S. Ishiwata, *Phys. Rev. B* **87**, 180501(R) (2013).
- [10] K. Kudo, M. Kobayashi, S. Pyon, and M. Nohara, *J. Phys. Soc. Jpn.* **82**, 085001 (2013).
- [11] K. Kudo, H. Ishii, M. Takasuga, K. Iba, S. Nakano, J. Kim, A. Fujiwara, and M. Nohara, *J. Phys. Soc. Jpn.* **82**, 063704 (2013).
- [12] S. Kitagawa, H. Kotegawa, H. Tou, H. Ishii, K. Kudo, M. Nohara, and H. Harima, *J. Phys. Soc. Jpn.* **82**, 113704 (2013).
- [13] L. R. Testardi, *Rev. Mod. Phys.* **47**, 637 (1975).
- [14] A. Gauzzi, S. Takashima, N. Takeshita, C. Terakura, H. Takagi, N. Emery, C. Hérold, P. Lagrange, and G. Louprias, *Phys. Rev. Lett.* **98**, 067002 (2007).
- [15] A. Gauzzi, N. Bendiab, M. d’Astuto, B. Canny, M. Calandra, F. Mauri, G. Louprias, N. Emery, C. Hérold, P. Lagrange, M. Hanfland, and M. Mezouar. *Pays. Rev. B* **78**, 064506 (2008).
- [16] L. E. Klintberg, S. K. Goh, P. L. Alireza, P. J. Saines,

- D. A. Tompsett, P. W. Logg, J. Yang, B. Chen, K. Yoshimura, and F. M. Grosche, *Phys. Rev. Lett.* **109**, 237008 (2012).
- [17] S. K. Goh, D. A. Tompsett, P. J. Saines, H. C. Chang, T. Matsumoto, M. Imai, K. Yoshimura, and F. M. Grosche, *Phys. Rev. Lett.* **114**, 097002 (2015).
- [18] W. C. Yu, Y. W. Cheung, P. J. Saines, M. Imai, T. Matsumoto, C. Michioka, K. Yoshimura, and S. K. Goh, *Phys. Rev. Lett.* **115**, 207003 (2015).
- [19] G. L. Pascut, K. Haule, M. J. Gutmann, S. A. Barnett, A. Bombardi, S. Artyukhin, T. Birol, D. Vanderbilt, J. J. Yang, S.-W. Cheong, and V. Kiryukhin, *Phys. Rev. Lett.* **112**, 086402 (2014).
- [20] T. Toriyama, M. Kobori, T. Konishi, Y. Ohta, K. Sugimoto, J. Kim, A. Fujiwara, S. Pyon, K. Kudo, and M. Nohara, *J. Phys. Soc. Jan.* **83**, 033701 (2014).
- [21] D. Ootsuki, S. Pyon, K. Kudo, M. Nohara, M. Horio, T. Yoshida, A. Fujimori, M. Arita, H. Anzai, H. Namatame, M. Taniguchi, N. L. Saini, and T. Mizokawa, *J. Phys. Soc. Jan.* **82**, 093704 (2013).
- [22] D. Ootsuki, T. Toriyama, S. Pyon, K. Kudo, M. Nohara, K. Horiba, M. Kobayashi, K. Ono, H. Kumigashira, T. Noda, T. Sugimoto, A. Fujimori, N. L. Saini, T. Konishi, Y. Ohta, and T. Mizokawa, *Rhys. Rev. B* **89**, 104506 (2014).
- [23] K. Takubo, R. Comin, D. Ootsuki, T. Mizokawa, H. Wadati, Y. Takahashi, G. Shibata, A. Fujimori, R. Sutarto, F. He, S. Pyon, K. Kudo, M. Nohara, G. Levy, I. S. Elfimov, G. A. Sawatzky, and A. Damascelli, *Phys. Rev. B* **90**, 081104(R) (2014).
- [24] K. -T. Ko, H. -H. Lee, D. -H. Kim, J. -J. Yang, S. -W. Cheong, M. J. Eom, J. S. Kim, R. Gammag, K. -S. Kim, H. -S. Kim, T. -H. Kim, H. -W. Yeom, T. -Y. Koo, H. -D. Kim, and J. -H. Park, *Nat. Commun.* 6:7342 doi: 10.1038/ncomms8342 (2015).
- [25] D. Ootsuki, K. Takubo, K. Kudo, H. Ishii, M. Nohara, N. L. Saini, R. Sutarto, F. He, T. Z. Regier, M. Zonno, M. Schneider, G. Levy, G. A. Sawatzky, A. Damascelli, and T. Mizokawa, *Phys. Rev. B* **90**, 144515 (2014).
- [26] G. Tunell and L. Pauling, *Acta Crystallogr.* **5**, 375 (1952).
- [27] W. J. Schutte and J. L. de Boer, *Acta Crystallogr. Sect. B: Struct. Sci., Cryst. Eng. Mater.* **44**, 486 (1988).
- [28] K. Reithmayer, W. Steurer, H. Schulz, and J. L. de Boer, *Acta. Crystallogr. Sect. B: Struct. Sci., Cryst. Eng. Mater.* **49**, 6 (1993).
- [29] The present syntheses did not provide metastable simple-cubic alloys Au-Te [30] and Au-Pd-Te [31], which demonstrate superconductivity. However, this is reasonable because the simple-cubic phase is never obtained unless rapid quenching is performed from the liquid phase at a rate of approximately 10^7 °C/s [31].
- [30] L. R. Newkirk and C. C. Tsuei, *Phys. Rev. B* **3**, 755 (1971).
- [31] W. Y. K. Chen and C. C. Tsuei, *Phys. Rev. B* **5**, 901 (1972).
- [32] N. Katayama, M. Uchida, D. Hashizume, S. Niitaka, J. Matsuno, D. Matsumura, Y. Nishihata, J. Mizuki, N. Takeshita, A. Gauzzi, M. Nohara, and H. Takagi, *Phys. Rev. Lett.* **103**, 146405 (2009).
- [33] See Supplemental Material at <http://link.aps.org/supplemental/10.1103/PhysRevB.93.140505> for electrical resistivity, the shielding diamagnetic signal, and x -dependent Wilson ratio.
- [34] C. J. Raub, V. B. Compton, T. H. Geballe, B. T. Matthias, J. P. Maita, and G. W. Hull, Jr., *J. Phys. Chem. Solids* **26**, 2051 (1965).
- [35] J. P. Carbotte, *Rev. Mod. Phys.* **62**, 1027 (1990).
- [36] W. L. McMillan, *Phys. Rev.* **167**, 331 (1968).
- [37] Here, we assumed that the value of χ ($= M/H$) for AuTe₂ is dominated by core diamagnetism because of the substantially reduced γ value in the monoclinic phase, and thus $\Delta\chi$ approximately represents Pauli paramagnetic susceptibility.
- [38] H. W. Myron, *Solid State Commun.* **15**, 395 (1974).
- [39] J. -P. Jan and H. L. Skriver, *J. Phys. F: Metal Phys.* **7**, 1719 (1977).

SUPPLEMENTAL MATERIALS

A. Structural phase transition

Figure S1 shows the electrical resistivity ρ for $\text{Au}_{1-x}\text{Pd}_x\text{Te}_2$. ρ shows a clear jump at the structural phase transition in the samples with $x = 0.40$ and 0.45 . The transition temperatures agree well with those determined from the magnetization. Consistent with the magnetization results, the transition temperature at which a jump is observed decreases upon Pd doping. A similar resistive anomaly was also reported in the high-pressure study of AuTe_2 [1].

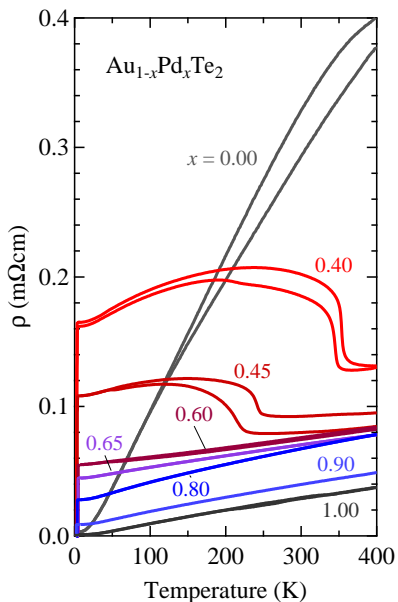


FIG. S1. Temperature dependence of electrical resistivity ρ for $\text{Au}_{1-x}\text{Pd}_x\text{Te}_2$.

B. Superconductivity

Figure S2 shows a dependence of electrical resistivity ρ and magnetization M on temperature for $\text{Au}_{1-x}\text{Pd}_x\text{Te}_2$ at low temperatures. The superconducting transition temperatures T_c determined from ρ and M are consistent with that of specific heat C .

C. Wilson ratio

Figure S3 shows a dependence of the Wilson ratio $\Delta\chi/\gamma$ (in units of $3\mu_B^2/\pi^2k_B^2$) on palladium content x for $\text{Au}_{1-x}\text{Pd}_x\text{Te}_2$. Here, $\Delta\chi$ corresponds to the difference in M/H between $x = 0.00$ (AuTe_2) and $x \neq 0.00$ ($\text{Au}_{1-x}\text{Pd}_x\text{Te}_2$) at 10 K. We assumed that the value of χ

($= M/H$) for AuTe_2 is dominated by core diamagnetism because of the substantially reduced γ value in the monoclinic phase, and thus $\Delta\chi$ approximately represents Pauli paramagnetic susceptibility.

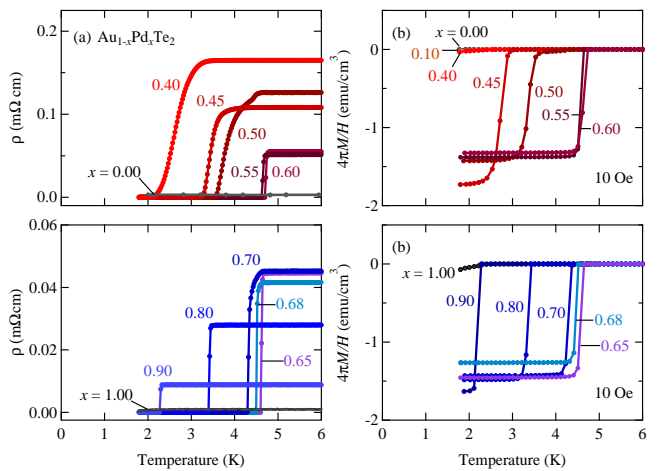


FIG. S2. (a) Temperature dependence of electrical resistivity ρ for $\text{Au}_{1-x}\text{Pd}_x\text{Te}_2$. (b) Temperature dependence of magnetization divided by magnetic field, M/H , in a magnetic field with 10 Oe for $\text{Au}_{1-x}\text{Pd}_x\text{Te}_2$ under zero-field cooling, in which no correction for the diamagnetizing field has been made.

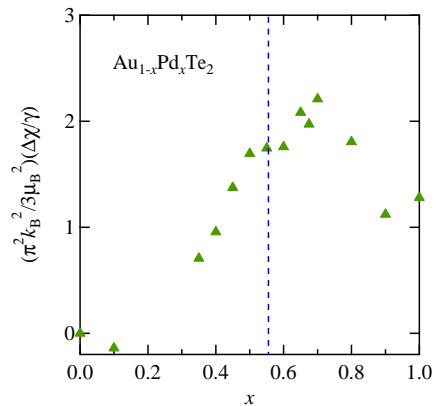


FIG. S3. Doping dependent Wilson ratio for $\text{Au}_{1-x}\text{Pd}_x\text{Te}_2$.

* kudo@science.okayama-u.ac.jp

† nohara@science.okayama-u.ac.jp

[1] S. Kitagawa, H. Kotegawa, H. Tou, H. Ishii, K. Kudo, M. Nohara, and H. Harima, J. Phys. Soc. Jpn. **82**, 113704 (2013).